NUMERICAL STUDY ON DENSITY AND SHAPE EFFECTS OF PROJECTILES FOR HYPERVELOCITY IMPACT

Masahide KATAYAMA*, Susumu TODA† and Seishiro KIBE†

*Structural Engineering Department, CRC Research Institute, Inc.
2-7-5, Minamisuna, Koto-ku, Tokyo 136, Japan
†National Aerospace Laboratory,
7-44-1 Jindaiji Higashi-machi, Chofu-shi, Tokyo 182, Japan

ABSTRACT

Christman et al. carried out two series of experiments of hypervelocity (6.6 km/s) impacts on semi-infinite aluminum targets: one is the test of density effect of projectile material, and the other is that of projectile shape effect. Both the conclusions contain important meaning from the standpoint of the protection and design from space debris impacts. In this study we performed a series of numerical analyses to simulate the experimental conditions and several extra cases, and proved that the shape of crater mainly depends on projectile density and a little bit upon projectile sound speed, and demonstrated that their conclusion on the shape effect of experimental results contains a misunderstanding.

1. INTRODUCTION

In order to protect the spacecrafts from the orbital space debris the stuffed Whipple bumper shield is usually adopted. However, the properties of the stuffing materials like Kevlar, Nextel, MLI, etc. are not known sufficiently from the viewpoint of hypervelocity impact problem. Therefore, if a certain well-known parameter is proved to be dominant factor for the cratering process of hypervelocity impact problem, it is very useful to predict the results of such complicated phenomena numerically. In this study the density is demonstrated to be the dominant factor of the current problem.

On the other hand the shape distribution of space debris in LEO is not known well at present. So, it is of great importance to investigate the projectile shape effect on the cratering process in the hypervelocity impact problem. Through the current study, the relationships of the projectile's '*l/d*' to the crater depth and volume are made clear by a series of numerical simulations.

2. REFERNCE EXPERIMENT

Christman et al. carried out two series of experimental tests of hypervelocity (6.6 km/sec) impacts on semi-infinite aluminum targets: one is the test of density effect of projectile material, and the other is that of projectile shape effect (Ref. 1). Their conclusion on density effect test is that the crater depth and volume for equal-mass spheres of various densities are given as a **convexly** monotone increasing function (Fig. 1-3).

The other conclusion on shape effect test is that the crater depth and volume for equal mass and various shapes are given as a **slightly concavely** monotone increasing function (Fig. 6-8).

3. NUMERICAL MODELING

Two-dimensional hydrocode: AUTODYN-2D™ was applied for the numerical simulation. All the calculations were made in the axisymmetric model. Though this hydrocode is a fully coupled computer program, only the multiple-material Eulerian processor was utilized all the time in this study. A number of equations of state (E.O.S.'s), i.e. Mie-Grüneisen type shock Hugoniot, Puff (Ref. 2) and Tillotson (Ref. 3), and constitutive equation, i.e. hydrodynamic, elastic-perfectly-plastic, Steinberg-Guinan (Ref. 4) and Johnson-Cook (Ref. 5), were used depending on the material and impact velocity. The details about these informations will be shown in next section. And as a fracture model we used the spall strength (negative maximum hydrostatic pressure) by which the numerical cell is triggered to be fractured instantaneously.

4. NUMERICAL AND EXPERIMENTAL RESULTS

Fig. 1 shows the comparison of created crater profiles between experiment (left-hand side) and calculation (right-hand side). Fig. 2 and 3 indicate the relationships of crater depth (& diameter) and volume to the

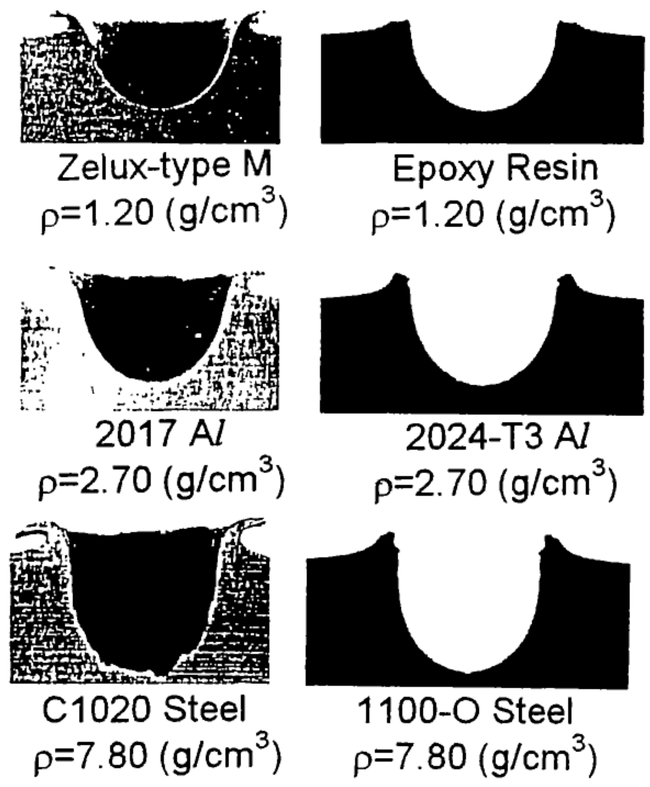

Fig. 1 Comparison of crater profiles between experiment and calculation.

Table 1 Material model and calculational results (1).

material	E.O.S.	C.M.	depth	diameter	volume
Epoxy	Shock	Hydro	1.50 cm	1.52 cm	6.47 cm^3
Plexiglas	Shock	Hydro	1.51 cm	1.51 cm	6.52 cm^3
Kevlar	Puff	Hydro	1.51 cm	1.52 cm	6.47 cm^3
2024-T3 Al	Shock	J-C	1.43 cm	1.48 cm	5.97 cm^3
2024-T3 Al*	Shock	J-C	1.50 cm	1.53 cm	6.74 cm^3

E.O.S.: equation of sate, C.M.: constitutive model
Hydro: Hydrodynamic, J-C: Johnson-Cook's Model

Table 2 Material model and calculational results (2).

material	E.O.S.	C.M.	depth	diameter	Volume
Kevlar	Puff	Hydro	1.30 cm	1.29 cm	4.69 cm^3
6061Al	Puff	E-P-P	1.52 cm	1.21 cm	4.89 cm^3
6061Al*	Puff	E-P-P	1.22 cm	1.38 cm	4.53 cm^3
6061Al*/Til.	Puff	E-P-P	1.22 cm	1.36 cm	4.52 cm^3

Til.: Tillotson's E.O.S., E-P-P: elastic-perfectly-plastic

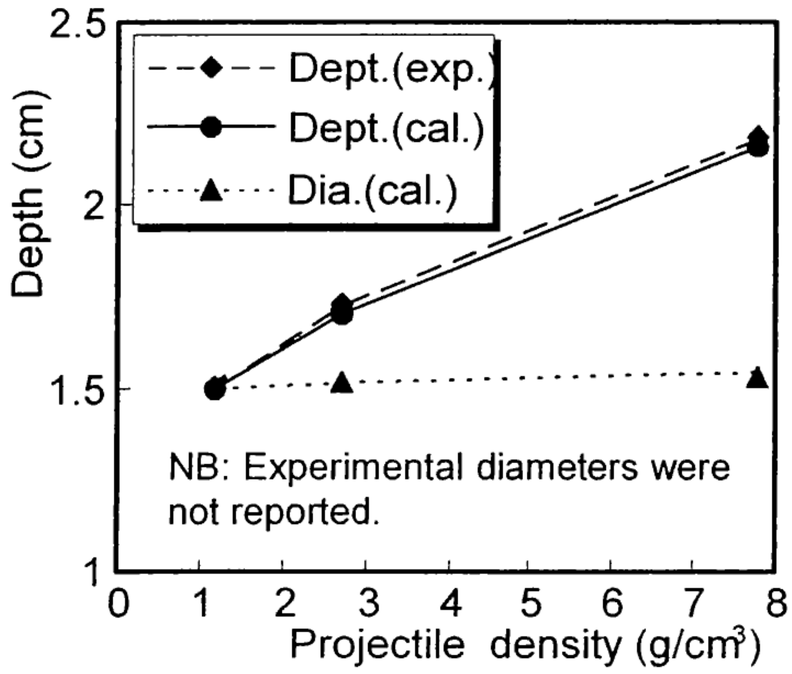

Fig.2 Variation of crater size with projectile density.

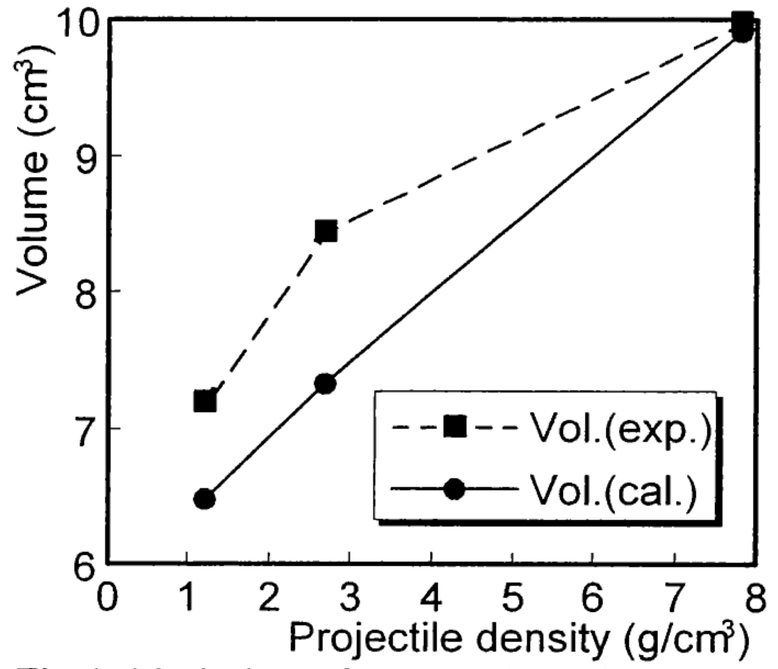

Fig.3 Variation of crater size with projectile density.

projectile density obtained by both experiment and calculation. As the properties of projectile materials used in the experiment were not known, the data guessed similar to each material was used in the calculation. Though all the targets were 1100-F Al in the experiment, they were assumed to be 1100-O Al in the calculation, as well as Epoxy Resin in place of Zelux-type M, 2024-T3 Al in place of 2017 Al and 1006 Steel in place of C1020 Steel. For all of the materials Mie-Grüneisen type shock Hugoniot E.O.S. was applied, Steinberg-Guinan constitutive model was applied for 1100-O Al, Epoxy Resin and 1006 Steel and Johnson-Cook model was for 2024-T3 Al. The density for each material in the calculation was assumed to have the same value in the corresponding experiment. These figures indicate fairly good agreements between experiment and calculation. Especially, should be noted that the diameter of craters in the calculation is not dependent upon the projectile density.

After confirming the coincidence between the experimental and calculational results, we carried out a series of numerical simulations to investigate if the projectile density is truly a dominant factor for the cratering process in this problem. That is, we performed five calculations in which E.O.S.'s and constitutive models of the properties are different but the densities are the same.

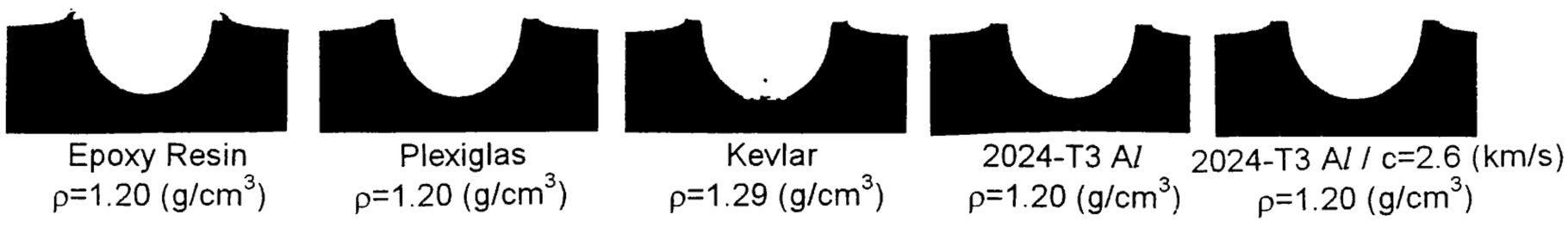

Fig.4 Equation of state effects on the crater profiles (calculated, impact velocity = 6.6 km/s, at 50 μs).

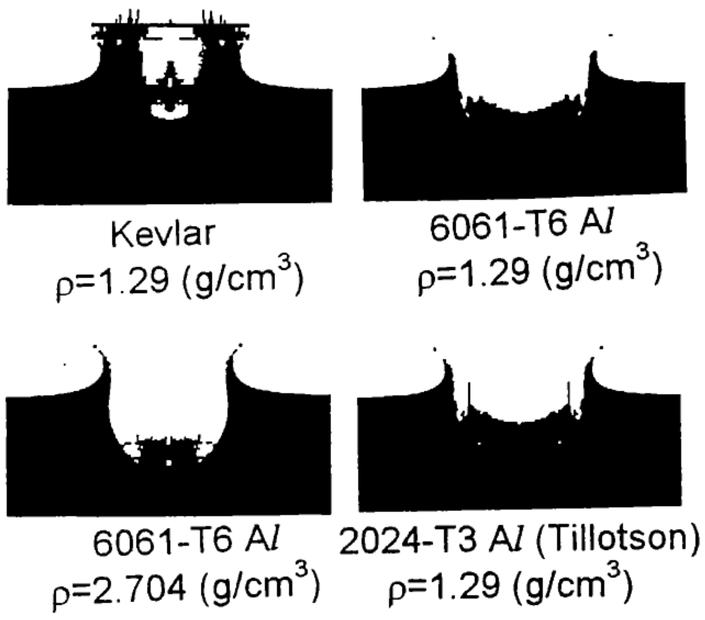

Fig. 5 E.O.S. effect on the crater and vaporized projectile profiles (calculated, impact velocity = 12 km/s, at 5 ms.

The applied material models and typical calculational results are summarized in Table 1 (Only the density of Kevlar is a true value.).

All the calculated depths, diameters and volumes indicate are comparable, but only the result of 2024-T3 A*l* are different a little bit from the other ones. The result of 2024-T3 A*l** is for the case of which only sound speed (c) is different form 2024-T3 A*l*; c=2.6 km/s. We can understand that the projectile density is the primary dominant factor and projectile sound speed is the secondary dominant factor for this problem through these analyses.

We carried out a series of calculations with 12 km/s impact velocities. As shock-induced vaporization will be occurred in this velocity region, we adopted Puff E.O.S. (Ref. 2) for projectile materials. The calculated profiles are shown in Fig. 5, the applied material models for projectiles and typical calculational results are summarized in Table 2. In the case of 6061 A*l**/Til. Tillotson E.O.S. was applied to the target material (2024-T3 A*l*), and in the cases of 6061 A*l** and 6061 A*l**/Til. the densities of projectiles were assumed to be 1.29 g/cm^3 equal with Kevlar's density. Only the result of 6061 A*l* is different from those of the other cases.

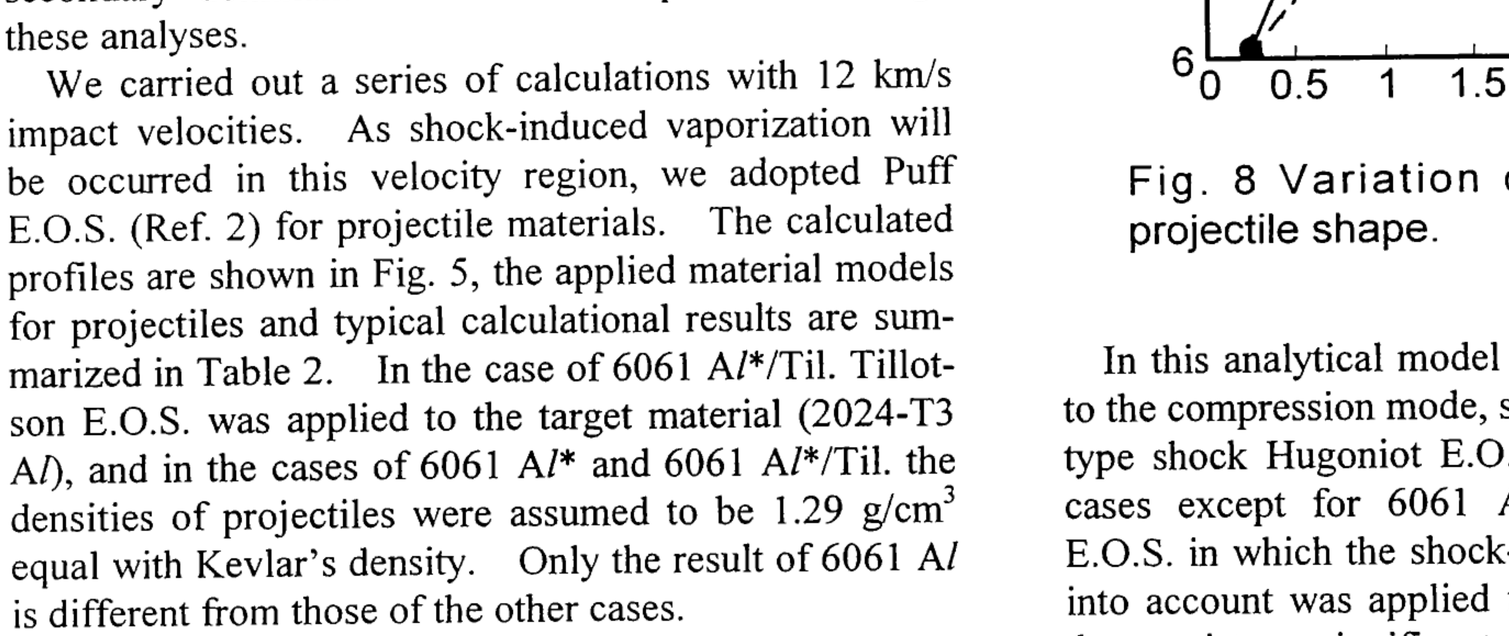

Fig. 6 Comparison of crater profiles between experiment and calculation.

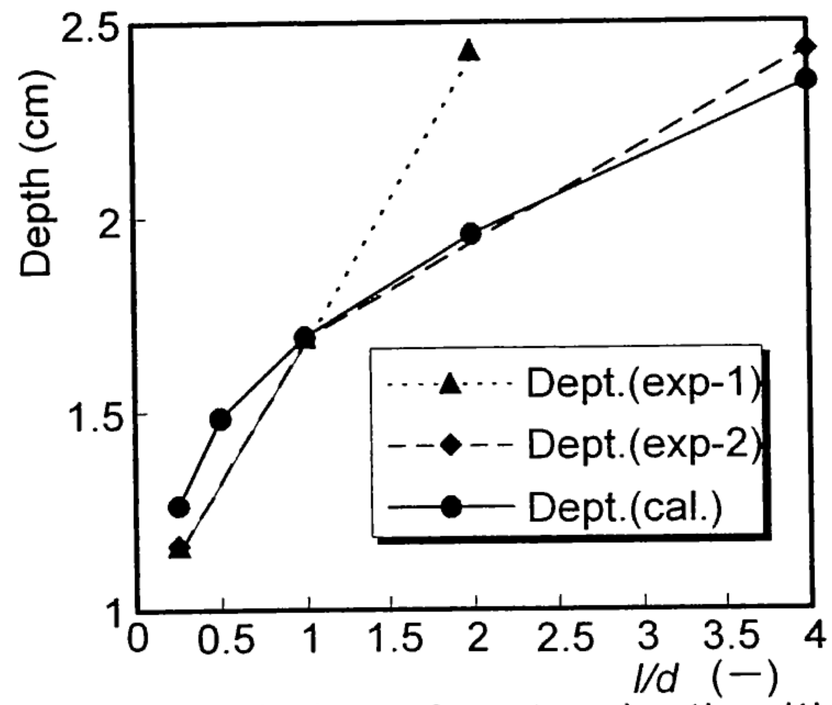

Fig. 7 Variation of crater depth with projectile shape.

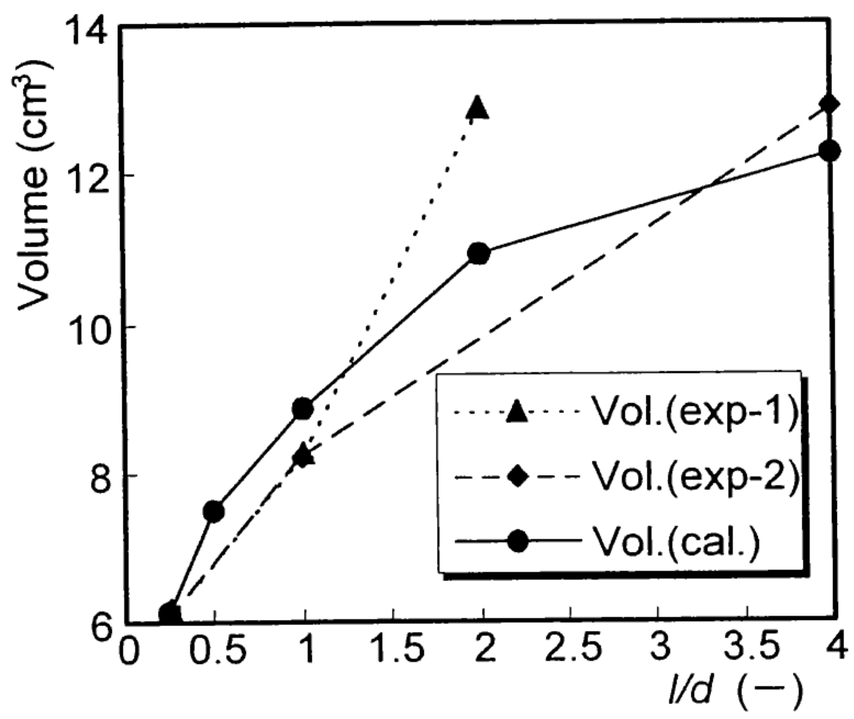

Fig. 8 Variation of crater volume with projectile shape.

In this analytical model the target is mainly subjected to the compression mode, so that we used Mie-Grüneisen type shock Hugoniot E.O.S. for the target in the three cases except for 6061 A*l**/Til. Although Tillotson E.O.S. in which the shock-induced vaporization is taken into account was applied for the target in the last case, there exist no significant differences in the result from 6061 A*l**, while the projectile is vaporized almost completely by the impact shock in every case. From these results we can see that the projectile density is also the primary dominant factor for the cratering process, while the vaporization process of projectiles is highly depend on other material properties.

Then we performed the analyses in order to investigate the shape effect of projectiles. Fig. 9 depicts the crater profiles which were created by the projectiles with same impact velocities 6.6 km/s) and same mass but different shapes. The upper results are experimental and the lower calculational. Reference paper (Ref. 1) describes that the last case's *l/d* of the projectile is 2.0, but the projectile's shape seems to be longer than this value judging from the figure, even if considering the tail part of the projectile. So we made a calculation the case with *l/d* = 4.0. The result has a much better agreement with the experimental result. Fig. 7 and 8 indicate the relationships of the crater depths and volumes with *l/d* of projectiles, respectively. The lines denoted 'exp-1' are based on the original data quoted in the reference, and the lines denoted 'exp-2' are plotted by using *l/d*=4 in place of *l/d*=2 in the experimental results. From these figures we can conclude that the reference paper contains a little misunderstanding about the value of *l/d*.

5. DISCUSSION AND CONCLUSIONS

The fact that the crater shape created on the semi-infinite target depends upon only the projectile density will enable us to estimate the damage of spacecraft much easier than the current procedure. Especially the stuffing and MLI materials adopted in the recent design for almost all the spacecrafts are not known about their dynamic material properties sufficiently, so that the efforts required for the material modeling will be reduced remarkably in the case of numerical simulation. In this study we performed a series of numerical analyses to simulate the experimental conditions and several extra cases, and proved that the shape of crater mainly depends on projectile density and a little bit upon projectile sound speed. Additionally we made a series of numerical simulations for the projectile with 12 km/s impact velocity, where shock-induced vaporization was taken into account. In this velocity region the density of projectile was still the dominant factor for the crater shape of the target, while the vaporization processes of projectiles were considerably different from each other depending on equations of state applied for the projectile materials.

The present study can be applicable only for semi-infinite target impact problem for itself, but one of the authors showed that thin target impact processes have also similar tendency with regard to the density effect (Ref. 6). Moreover, this result is reasonable judging from the theory that the impact pressure of the projectile on the rigid wall is calculated by the product of shock impedance and impact velocity: $\rho c \times u$, where ρ is density, c is sound (shock) velocity and u is impact velocity of the projectile.

The other conclusion on shape effect test is that the crater depth and volume for equal mass and various shapes are given as a **slightly concavely** monotone increasing function. Our numerical analysis results told us that the crater depth and volume for equal mass and various shapes also given as a **convexly** monotone increasing function like the density effect. This difference might be caused by their misunderstanding of the longest projectile's *l/d*, taking 2.0 for 4.0.

On the other hand Gehring, a co-author of Christman's paper, concluded in a famous and useful textbook (Ref. 7) that the result of the projectile's shape effect test was significant in military applications where impact velocities were below 10 km/sec, however, for meteoroid impacts, it was reasonable to assume that the particles were approximately spherical and, consequently, that shape was not a governing factor in damage. However, since the shape distribution of orbital space debris is not known well, we think, it is important to assess the debris shape effect in protection design.

REFERENCES

1. D. R. Christman, J. W. Gehring, C. J. Maiden and A. B. Wenzel, "Study of the Phenomena of Hypervelocity Impact," *GM TR63-216*, 1963.

2. L. H. Bakken et al., "An Equation-of-State Handbook," Sandia Laboratories, Livermore, *SCL-DR-68-123*, 1969

3. J. H. Tillotson, "Metallic Equations of State for Hypervelocity Impact," General Atomic, *GA-3216*, 1962

4. D. J. Steinberg et al., "A Constitutive Model for Metals Applicable at High-Strain Rate," *J. Appl. Phys.*, 51, 1980

5. G. R. Johnson et al., " A Constitutive Model and Data for Materials Subjected to Large Strains, High Strain Rates and High Temperatures," *Proc. 7th Int. Symp. on Ballistics*, Hague, 1983

6. K. Shiraki, M. Harada, S. Terada and M. Katayama, "Hydrocode Simulation for Space Debris Impact," *Proc. of the 40th Space Sciences and Technology Conference*, 1996 (in Japanese)

7. J. W. Gehring Jr. (Ed. By R. Kinslow), "Chapter IX Engineering Considerations," *High-Velocity Impact Phenomena*, Academic Press, 1970